Finite element modelling of incompressible problems in geomechanics

Dieter Stolle
McMaster University, Hamilton, Ontario, Canada
Issam Jassim & Pieter Vermeer
Institut für Geotechnik – Universität Suttgart, Stuttgart, Germany

ABSTRACT
Geotechnical problems such as landslides, mud flows and ice flows are often modeled assuming incompressibility and nonlinear visco-elastic/plastic material behavior. This paper examines low order finite element solution techniques for incompressible problems within the context of explicit matrix free algorithms. It is shown that it is necessary to introduce volumetric strain enhancement, as well as the conditioning of creep/plastic strains by allowing a small amount of compressibility to avoid predicting unrealistic pressures. The emphasis in this paper is on the creep of large ice masses.

RÉSUMÉ
Les problèmes géotechniques tels que les glissements des terres et les coulées de boue et de glace sont souvent modélisés en supposant un comportement incompressible, no linéaire et visqueux-élastique/plastique des matériaux. Ce papier examine les solutions techniques en éléments finis d'ordre réduit pour les problèmes incompressibles dans le cadre de la matrice explicite algorithmes libres. Il est démontré qu'il est nécessaire d'introduire une amélioration de la déformation volumétrique, ainsi que le conditionnement des déformations dues au fluage / plastique en permettant une petite compressibilité pour éviter une prévision irréaliste des pressions. L'accent mis dans ce document est sur le fluage de grandes masses de glace.

1 INTRODUCTION

Considerable progress has been made since the 1970's in developing finite element models for geomechanics applications. The methodology lends itself well to stress and groundwater flow analyses, including the coupling of soil-water interaction. Up until the late 1980's, attention focused on introducing high order elements, as well as providing better constitutive relations. More recent developments of the methodology have however moved away from high order to low order finite element implementations to take advantage of more versatility offered by adaptive mesh formulations and material point method applications.

While the practicing engineer need not be concerned with computational details, he (or she) should be familiar with the limitations embedded in the low order models. The objective of this paper is to examine two solution procedures for tackling incompressible problems within the context of explicit matrix free algorithms. The emphasis in this paper is on slope creep, where incompressibility of the creep strains create problems with regard to locking and steady-state pressure predictions.

2 INCENTIVE FOR LOW ORDER ELEMENTS

In recent years, matrix-free finite element techniques have received considerable attention for the solution of three dimensional problems involving non-structured meshes and large deformations or impact problems (Zienkiewicz et al.1998). Among the evolving techniques is the material point method where the focus is on material points, which carry information regarding material state through a stationary mesh (Wieckowski et al. 1999). An important task with this procedure is the mapping of information between the computational mesh and material points. For problems involving dynamics, this can be best accomplished with low order interpolation functions.

2.1 Drawbacks with high order elements

For many standard applications, high order elements have proven to perform better than low order elements. There are, however, situations such as shown in Figure 1, where higher order elements have problems. This figure shows the predicted horizontal surface velocity variation along the length of Barnes Ice Cap on Baffin Island Canada, along with the high order finite element mesh. To maintain the same number of degrees of freedom, four low order elements were used for each high order element. To achieve reasonable surface velocities it was necessary to model sufficient basal sliding between the 11 and 34 km section. A reduction in sliding resistance (normalized but same scale as velocity) is also shown.

For this series of simulations, the linear displacement element provided more realistic velocities. One clearly observes that predictions when using the high order mixed elements (quadratic velocity and linear pressure) are very different around the 17 km point. The high velocities are attributed to the inability of the high order interpolation functions to properly accommodate the variation in sliding resistance, as well as the severe conditions imposed by incompressibility of flow. Improvements in the high order element solution are possible by reducing the rate of resistance reduction at

the base, as well as incorporating some compressibility into the flow field.

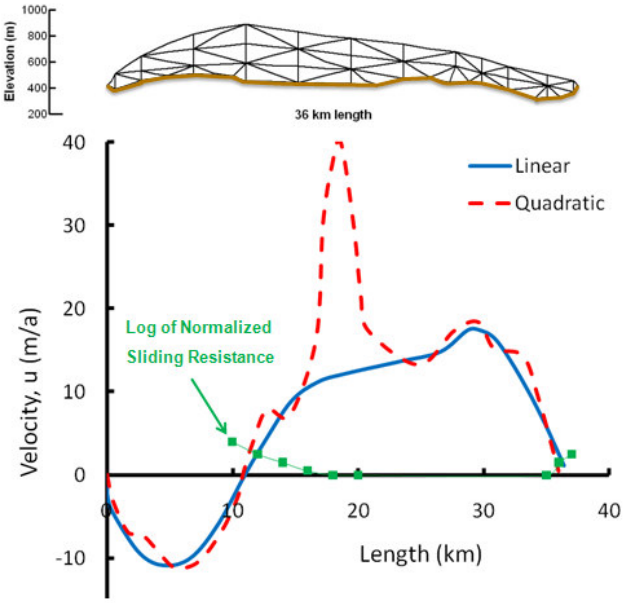

Figure 1. Prediction of surface velocities (Stolle 1982)

2.2 Challenges with low order elements

If we do a dimensional analysis, we quickly come to the conclusion that pressure (implying mean normal stress) should be interpolated one order less than the displacement or velocity field. For various reasons, researchers prefer having equal order approximations, which however require special algorithms.

Implementation of linear, equal-order displacement-pressure elements poses challenges, as low order elements are known to lock and pressure distributions display spurious spatial oscillations when material behaviour is near incompressible and standard Galerkin procedures are used to develop the matrix equations.

Let us consider a system of equations, say for glacier flow, where velocities **v** and pressures **p** are interpolated:

$$\begin{bmatrix} \mathbf{K} & \mathbf{Q} \\ \mathbf{Q}^T & \mathbf{0} \end{bmatrix} \begin{Bmatrix} \mathbf{v} \\ \mathbf{p} \end{Bmatrix} = \begin{Bmatrix} \mathbf{f} \\ \mathbf{0} \end{Bmatrix} \qquad [1]$$

Without going into details, the first line is associated with equilibrium or momentum balance and the second with constraint equations due to volumetric strain-pressure relation. In order to have a non-singular matrix, we require fewer constraint equations than equilibrium equations; see for, e.g., Wan (2002). This is best achieved by using lower order interpolation for pressure. Alternatively, a common technique to convert the saddle point to a parabolic problem, artificial compressibility is often introduced to remove the **0**. While this is useful for higher order elements, it is most often not sufficient when adopting linear interpolation. Stabilization can however be achieved by using iterative techniques involving the partitioning and correcting the displacement and velocity field thorough stepwise explicit-implicit uncoupled time-stepping; see, e.g., Zienkiewicz and Taylor (1991), and Nithiarasu (2006).

3 FIELD EQUATIONS

Two approaches are investigated here for finding quasi-static equilibrium solutions that are consistent with incompressible flow fields of creeping bodies. We assume that the flow field can be obtained by allowing the body to creep from an elastic state of stress to one that is dominated by the creep properties. We are looking for a large deformation solution where the influence of elastic deformations is negligible. The approaches that we propose here belong to the class procedures that are sometimes referred to as methods of successive approximation.

In the first procedure, we use an explicit dynamic solver to iterate. The second procedure is based on a quasi-static initial strain algorithm. In order to deal with incompressibility, the volumetric strains are enhanced (imitating a mixed formulation) in both approaches.

3.1 Momentum balance

For the first part of the paper, indicial notation is adopted and it is assumed that tension is positive. The symbol p denotes the mean normal stress (spherical stress) and σ_{ij} is the stress, which can be decomposed into deviatoric $\tau_{ij} = \sigma_{ij} - \delta_{ij} p$ and spherical stress components. The spherical stress is the negative of pressure. Given that ρ is density and the corresponding velocity $v_i = \dot{u}_i$ is the derivative of displacement u_i with respect to time (denoted by a superposed dot), dynamic equilibrium for the x_i direction is expressed in differential form as:

$$\rho \dot{v}_i = \sigma_{ij,j} + \rho g_i \qquad [2]$$

where g_i is acceleration, and $(\ )_{,i}$ refers to differentiation with respect to x_i .

3.2 Kinematic relation

The total strain ε_{ij} of a creeping solid is represented by

$$\varepsilon_{ij} = \frac{1}{2}\left(u_{i,j} + u_{j,i}\right) \qquad [4]$$

It is often more convenient to use matrix notation with $\boldsymbol{\varepsilon} = \mathbf{L}\mathbf{u}$, in which $\boldsymbol{\varepsilon}$ is the strain, **u** is the displacement vector and **L** is the linear differential operator. When dealing with the vector form is common to use engineering strain where for shear we have $\gamma_{ij} = 2\varepsilon_{ij}$ when $i \neq j$. The strain rate is given by $\dot{\varepsilon}_{ij}$.

3.3 Creep law

Allowing for some compressibility in the flow field, the creep strain rate $\dot{\varepsilon}_{ij}^c$ may be expressed as:

$$\dot{\varepsilon}_{ij}^c = \frac{\nu_c}{2\mu}\sigma_{kk}\delta_{ij} + \frac{\sigma_{ij}}{2\mu} \;\rightarrow\; \tau_{ij} = 2\mu\dot{\varepsilon}_{ij}^c \quad \text{for } \nu_c \rightarrow \frac{1}{2} \qquad [5]$$

where μ is a stress-dependent viscosity given by

$$\mu = \frac{1}{3}\frac{\sigma_e}{\dot{\varepsilon}_e^c} \quad \text{with} \quad \dot{\varepsilon}_e^c = A\sigma_e^m \qquad [6]$$

in which A and m are creep parameters, δ_{ij} is the Kronecker delta and $\dot{\varepsilon}_e = \sqrt{2/3\,\dot{\varepsilon}_{ij}\dot{\varepsilon}_{ij}}$ and $\sigma_e = \sqrt{3/2\,\tau_{ij}\tau_{ij}}$ are equivalent strain rate and equivalent stress, respectively. While the viscosity is analogous to shear modulus, the parameter ν_c is a 'Poisson's ratio' for the creep strain field. It will be demonstrated that some compressibility is required to help stabilize the pressure field.

3.4 Constitutive law

Within the context of solid mechanics, we can invoke the Prandtl-Reuss approximation to relate changes in stress $\Delta\boldsymbol{\sigma}\left(=\boldsymbol{\sigma}_1 - \boldsymbol{\sigma}_0\right)$ to changes in total strain $\Delta\boldsymbol{\varepsilon}$ at time t_1 via

$$\Delta\boldsymbol{\sigma} = \mathbf{D}\left(\Delta\boldsymbol{\varepsilon} - \Delta t\dot{\boldsymbol{\varepsilon}}^c\right)_0 \qquad [7]$$

where **D** is the elastic constitutive matrix, $\dot{\boldsymbol{\varepsilon}}^c$ is the creep strain rate given by Eq. 5 and Δt is the actual time step.

The field equations that have been listed correspond to those encountered in small deformation theory. If one compares these equations to those for thick viscous fluids, one can exploit the similarities. The equations for solids are usually Lagrangian in nature with those for fluids being Eulerian. Nevertheless, the flow and stress fields corresponding to a creeping body can be obtained by not updating geometry and the location of particles, and successively determining changes in stress. The flow solution is attained when the changes in stress vanish.

4 DYNAMIC TIME MARCHING ALGORITHM

We now turn to the matrix notation and begin by writing the weak form for the momentum equation of a solid bound by surface *S* and occupying volume *V*,

$$\int_V \delta\mathbf{u}^T\rho\,\dot{\mathbf{v}}dV + \int_V \delta\boldsymbol{\varepsilon}^T\boldsymbol{\sigma}\,dV - \int_V \delta\mathbf{u}^T\rho\,\mathbf{g}dV - \int_S \delta\mathbf{u}^T\mathbf{t}dS = 0 \qquad [8]$$

The tensor variables **t**, **b**, **ε** and **σ** take on the familiar meanings of surface traction, body force, strain and stress, respectively, with the δ implying a virtual quantity Given that the displacement field is approximated as $\mathbf{u} = \mathbf{N}\mathbf{a}$ where **N** represents interpolation matrix and **a** nodal displacements, we can define the strain as $\boldsymbol{\varepsilon} = \mathbf{B}\mathbf{a}$, with $\mathbf{B} = \mathbf{L}\mathbf{N}$ being the kinematic matrix. If we denote the nodal velocity by $\mathbf{v} = \dot{\mathbf{a}}$, Eq. 8 can written as

$$\int_V \rho\mathbf{N}^T\mathbf{N}dV\dot{\mathbf{v}} = \int_V \mathbf{N}^T\rho\,\mathbf{g}dV + \int_S \mathbf{N}^T\mathbf{t}\,dS - \int_V \mathbf{B}^T\boldsymbol{\sigma}dV \qquad [9]$$

or $\mathbf{M}\dot{\mathbf{v}} = \mathbf{R}$ where $\mathbf{R}\left(=\mathbf{F}^e - \mathbf{F}^i\right)$ is the out-of-balance force with $\mathbf{F}^e$ representing the external loading and $\mathbf{F}^i$ the internal forces due to stresses. The consistent mass matrix **M** is usually converted to a lumped mass matrix to eliminate computationally intensive matrix inversions. For details the reader is referred to Zienkiewicz and Taylor (1989).

We now take Eq. 9 and express it in difference form as

$$\mathbf{M}\frac{\mathbf{v}_1 - \mathbf{v}_0}{\Delta t} = \mathbf{R}_0 + \mathbf{C}_0 \qquad [10]$$

in which $\mathbf{C}_0$ represents the creep loading given by

$$\mathbf{C}_0 = \int_V \mathbf{B}^T\mathbf{D}\Delta t\left(\dot{\boldsymbol{\varepsilon}}^c\right)_0 dV \qquad [11]$$

Subscripts 0 and 1 for denote quantities such as nodal velocity **v** at the beginning and end of the interval, respectively. The displacement corresponding to the end of time step Δt is determined by $\mathbf{a}_1 = \mathbf{a}_0 + \Delta t\,\mathbf{v}_1$. This implies that the changes in stress $\Delta\boldsymbol{\sigma}$ depend on the stain increment $\Delta\boldsymbol{\varepsilon}$ that is determined from $\Delta\mathbf{a} = \Delta t\,\mathbf{v}_1$, and the stress and strain at time $t_1 = t_0 + \Delta t$ are given by $\boldsymbol{\sigma}_1 = \boldsymbol{\sigma}_0 + \Delta\boldsymbol{\sigma}$ and $\boldsymbol{\varepsilon}_1 = \boldsymbol{\varepsilon}_0 + \Delta\boldsymbol{\varepsilon}$.

Owing to the explicit time stepping operations, the maximum permissible time step is limited by the creep requirement

$$\Delta t < \Delta t_{cr} = \frac{4\left(1+\nu\right)}{3Em}\frac{\sigma_e}{\dot{\varepsilon}_e^c} \qquad [12]$$

with *E* being the elastic modulus and ν the Poisson's ratio. To properly capture the initial transient behaviour, we often specify $\Delta t = \alpha\,\Delta t_{cr}$ with $\alpha << 1$. The reduction factor α = 0.01 was selected in this study. The factor can be increased as the creep proceeds. To ensure that the algorithm remains stable due to the wave propagation and that the dynamic response is properly captured, the time step is also limited by the requirement

$$\Delta t < \text{minimum}\left(\frac{h^2\rho}{2K}\right) \qquad [13]$$

with *h* being a characteristic element dimension, which in this study was taken as twice the area of an element divide by the longest side. Minimum implies that the element that provides the smallest time step controls.

At this point it is prudent to examine what the algorithm is doing. Strictly speaking, the inertial forces play a minor role and are present only to detect changes in the residual load vector resulting from creep. These creep forces result in changes in velocity, which in turn lead to displacements that cause further changes in stress. Eventually, the velocities do not change and $\Delta\boldsymbol{\varepsilon} \to \Delta t\dot{\boldsymbol{\varepsilon}}^c$, which in turn implies that the stresses remain constant.

5 QUASI STATIC APPROACH

For materials that creep rapidly, steady state flow fields can also be achieved by using initial strain procedures. In this section, we immediately go to the discretized equivalent for equilibrium, dropping the inertial term appearing in Eq.'s 9 an 10. The quasi-static equilibrium for time t_1 is written as:

$$\mathbf{F} - \int_V \mathbf{B}^T \left(\boldsymbol{\sigma}_0 + \Delta\boldsymbol{\sigma}\right) dV = \mathbf{0} \qquad [14]$$

which together with Eq. 7 yields:

$$\int_V \mathbf{B}^T\mathbf{D}\mathbf{B}\, dV\Delta\mathbf{a} = \left(\mathbf{F} - \int_V \mathbf{B}^T\boldsymbol{\sigma} dV\right)_0 + \int_V \mathbf{B}^T\mathbf{D}\Delta t\left(\dot{\boldsymbol{\varepsilon}}^c\right)_0 dV \qquad [15]$$

or given the initial stiffness matrix **K**, $\mathbf{K}\Delta\mathbf{a} = \mathbf{R}_0 + \mathbf{C}_0$. An examination of Eq. 15 indicates that creep continuously introduces an initial load to the system, but as steady-state is reached $\Delta\boldsymbol{\sigma} \to \mathbf{0}$ due to $\Delta\boldsymbol{\varepsilon} \to \Delta t\dot{\boldsymbol{\varepsilon}}^c$ as we observed previously. Equation 15 requires matrix operations. These can be avoided by using the relaxation. Following Nithiarasu (2008), who made use of algorithms for fluid mechanics, we write

$$\mathbf{M}\frac{\left(\mathbf{a}_0^{n+1} - \mathbf{a}_0^n\right)}{\Delta t_e} = \left(\mathbf{F} + \int_V \mathbf{B}^T\mathbf{D}\Delta t\left(\dot{\boldsymbol{\varepsilon}}^c\right) dV\right)_0 - \int_V \mathbf{B}^T\mathbf{D}\Delta\boldsymbol{\varepsilon}_0^n dV \qquad [16]$$

where **M** is a 'lumped mass matrix' consistent with

$$\mathbf{M} = \int_V \rho\mathbf{N}^T\mathbf{N}\, dV \qquad [17]$$

It is important to realize that the term on the left hand side is introduced only to iterate and does NOT represent inertia. The objective is to have $\mathbf{a}_0^{n+1} - \mathbf{a}_0^n \to \mathbf{0}$ Since the inertia is not important and ρ is an 'apparent density' determined for each element to ensure the same critical time step according to $\rho = 2K\Delta\bar{t}_{cr}/h^2$ where *K* is the bulk modulus and $\Delta\bar{t}_{cr}$ represents a critical time step with *h* being the characteristic element dimension. The time step Δt_e takes the role of a counter with the superscript *n*+1 referring to the value of a variable at 'iteration time' $t^{n+1} = t^n + \Delta t_e$. It should be noted that all the physics is contained on the right hand side of the Eq. 16, with the permissible changes in displacement depending on the left hand side. Given that we can select optimum densities, we can specify $\Delta t_e = 1$. A critical time step of Δt_{cr} = 1.05 was found to work well. The approach suggested here for determining an optimum left hand side is slightly different from that recommended by Nithiarasu (2008).

Once again it is prudent to examine what is happening. According to Eq. 16, for a given load **F** and creep force $\mathbf{C}_0$, which is kept constant during a sequence of iterations corresponding to keeping time constant as denoted by the subscript, we calculate a correction to the displacement $\Delta\mathbf{a}$, which in turn leads to a change in the strain increment; i.e., the update strain increment is $\Delta\boldsymbol{\varepsilon}_0^{n+1} = \Delta\boldsymbol{\varepsilon}_0^n + \mathbf{B}\left(\mathbf{a}_0^{n+1} - \mathbf{a}_0^n\right)$. We keep on updating $\Delta\boldsymbol{\varepsilon}_0$ until the changes in displacement are sufficiently small; i.e., the tolerance $\eta > \left\|\mathbf{a}_0^{n+1} - \mathbf{a}_0^n\right\| / \left\|\mathbf{a}_0^{n+1}\right\| \to 0$. At this point, the stresses are updated using Eq. 7 and the process is repeated with a new creep loading. The initial value $\Delta\boldsymbol{\varepsilon}_0^0$ is **0** for each time step.

6 MITIGATING LOCKING

If one examines the changes in mean stress for mixed formulations, one has weighted residual for change in mean stress Δp:

$$\int_V \delta p\left(\Delta u_{j,i} - \frac{\Delta p}{K}\right) dV = 0 \qquad [18]$$

with the δ implying a weighting function. The significance of this equation is that incremental pressure as a result of incremental volumetric strain is NOT satisfied point wise, but rather in a weighted residual sense. For the procedures described in this paper, it is necessary to enhance the incremental volumetric strain $\Delta\varepsilon_v$ or strain rate in a similar manner. This can be accomplished if we write

$$\int_V \delta\varepsilon_v \left(\Delta u_{j,i} - \Delta\varepsilon_v\right) dV = 0 \qquad [19]$$

where $\Delta\varepsilon_v$ is discretized.

From a practical point of view the approach proposed by Detournay and Dzik (2006), can be easily implemented. This technique involves first determining the strain rates for each element in the usual manner and partitioning them into volumetric $\dot{\varepsilon}_v = \dot{\varepsilon}_{kk}$ and deviatoric $\dot{\varepsilon}_{ij}^d = \dot{\varepsilon}_{ij} - \delta_{ij}\dot{\varepsilon}_v/3$ components. The nodal volumetric strain rate for a node is determined by volume averaging the strain rates of elements attached to the node via

$$\dot{\bar{\varepsilon}}_v = \frac{\sum_k \left(\dot{\varepsilon}_v V\right)_k}{\sum_k \left(V\right)_k} \qquad [20]$$

where the sum is over all elements k attached to the node. Once the average volumetric strain rate is determine for each node, the average volumetric strain rate $\overline{\dot{\varepsilon}_v}$ for an element is determined by averaging the values of those nodes attached to the element.

$$\overline{\dot{\varepsilon}_v} = \frac{1}{d}\sum_k \dot{\varepsilon}_v \qquad [21]$$

with d being the number of vertices. The enhanced strain rate for an element now becomes $\dot{\varepsilon}_{ij} = \dot{\varepsilon}^d_{ij} + \delta_{ij}\overline{\dot{\varepsilon}_v}/3$.

7 DOUBLE SLOPE EXAMPLE

The example provided in this section is fairly simple but clearly highlights the problems that one has when modelling problems where the material behaviour is incompressible. Referring to Figure 2, a creeping, isothermal slope is considered, in which symmetry exists at x = 0 m (roller boundary). The numerical problem arises due to the break in slope along the base where the ice is fully fixed. While the finite element (research) code has been developed to handle nonlinear flow conditions, a linear rule is considered here with A = 0.001 (kPa-a)$^{-1}$. The unit weight of the material is 10kN/m^3, and the elastic modulus and Poisson's ratio were assumed to be 1000 MPa and 0.3, respectively. Simulations were also completed for higher elastic modulus with little change in the predicted flow field. The analyses were completed by starting from an elastic state of stress and allowing the body to creep to a state of stress that is consistent with the steady state flow field.

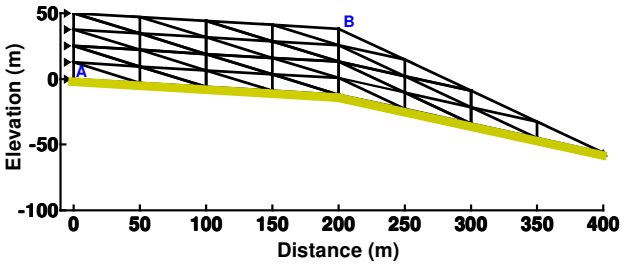

Figure 2. Finite element mesh for double slope.

Five cases were considered using the quasi static approach: Cases 1 and 2 assumed ν_c=0.5 and used quasi-static analysis without and with enhanced volumetric strains, respectively; Case 3 assumed ν_c=0.495 and was performed with quasi-static analysis and enhanced volumetric strains; and Cases 4 and 5 adopted the relaxation technique and ν_c=0.495 without and with enhanced volumetric strains, respectively. The dynamic analysis assumed the same conditions as given for Case 5. A constant time step of 0.0001 day was adopted for the dynamic scheme, whereas for the quasi static approach it was monitored using Eq. 12, with a convergence tolerance η = 0.0001. The mean stress history is shown for point A, bottom left, to examine stabilization of the spherical stress (pressure), with horizontal velocity history shown for point B to study the mitigation of locking.

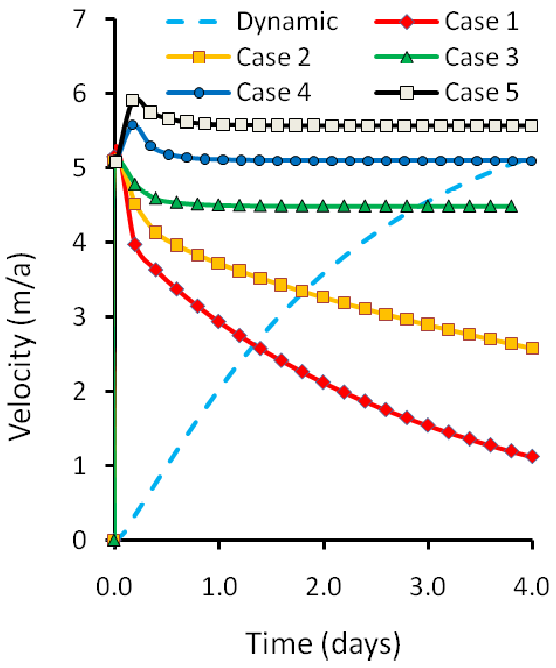

Figure 3. Horizontal velocity history for point B.

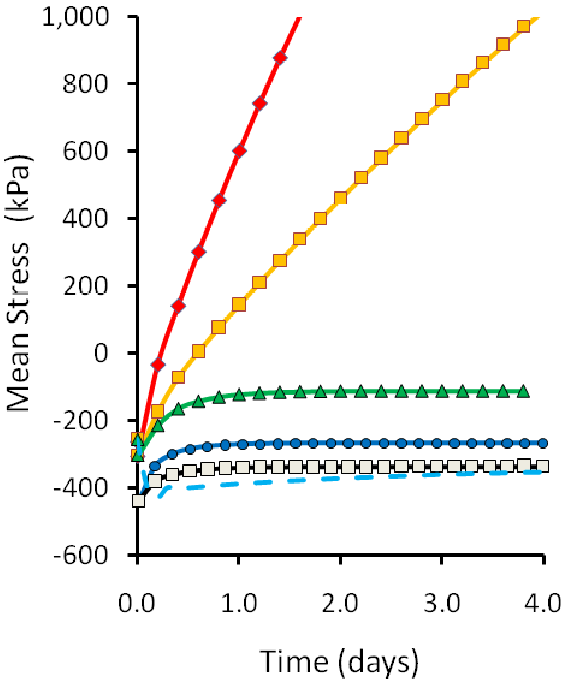

Figure 4. Mean stress history for point A (legend above).

An examination of the velocity histories in Figure 3 clearly shows that the traditional quasi static approach without conditioning is subject to locking. The steady state solution using high order elements with quadratic interpolation yields a horizontal velocity of the crest approaching 5.9 m/a. Conditioning by using enhanced volumetric strains improves the predictions, but the introduction of a small amount of compressibility into the creep strains is required to further decrease locking and improve the velocity. An examination of the mean stresses Figure 4, reveals that the traditional approach predicts stresses that are unrealistic, even with strain enhancement. More realistic values are obtained by allowing for some compressibility of the flow field, although the mean stresses are still inaccurate. To achieve reasonable values, it is necessary to use an iterative solver, in which the solution progressively develops. This is most likely attributed to strain enhancement being directly incorporated into the iterative process as the matrix-free solution is evolving. For traditional approaches involving matrix operations, the strain enhancement is applied less frequently. The dynamic procedure provides a different history, as might be expected, but the steady-state predictions are similar.

At this point we examine the pressure and maximum shear stress distributions shown in Figures 5 and 6, respectively, to see impact of using matrix-free technique. Red denotes high values with dark blue corresponding to zero. Both cases here accommodate enhanced volume strains and compressibility of the flow field. A close scrutiny of the results reveals that smoother transitions are obtained when iterating. Furthermore, the variation in pressure and shear stress is captured better for Case 6 than Case 3 when compared with higher order solutions.

Case 3

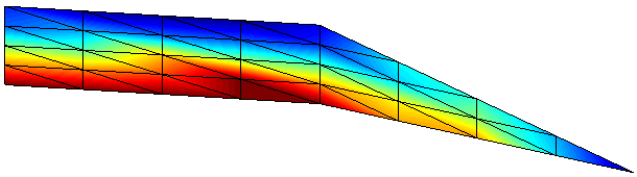

Case 5

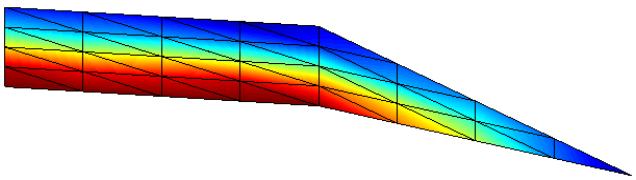

Figure 5. Comparative pressure variations (0 to 400 kPa).

8 CONCLUDING REMARKS

Two procedures for analyzing boundary-valued problems with low order finite elements, in which the material behaviour is incompressible, were investigated. It is observed that good quality predictions are possible provided that the volumetric strains are enhanced, some compressibility is allowed in the flow field and matrix-free iterative solution techniques are adopted. Of significance is the observation that the predictions could be achieved without introducing pressure as a primitive variable.

Case 3

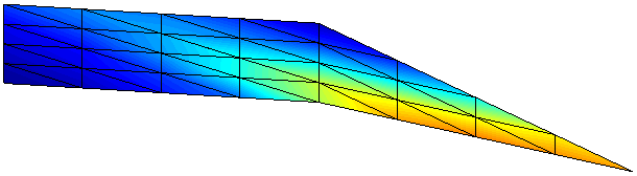

Case 5

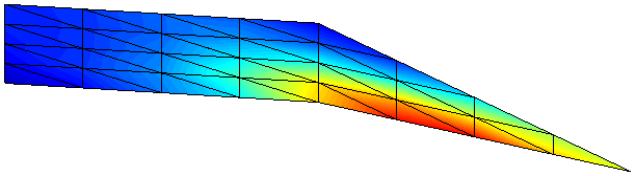

Figure 6. Maximum shear stress variations (0 to100 kPa).

ACKNOWLEDGEMENTS

Partial funding for this research was provided by the Natural Science and Engineering Research Council of Canada. The space and resources provided by the Institut für Geotechnik, Universität Suttgart is very much appreciated.

REFERENCES

Detournay, C. and Dzik, E. 2006. Nodal mixed discretization for tetrahedral elements. 4th Int. FLAC Symposium on Numerical Modeling in Geomechanics. Hart and Varona (eds.) Paper: 07-02© 2006 Itasca Consulting Group, Inc., Minneapolis.

Malvern, L. E. 1969. Introduction to the mechanics of a continuous medium, Prentice-Hall Inc., New Jersey.

Nithiarasu, P.A. 2006. Matrix free fractional step method for static and dynamic incompressible solid mechanics. Int. Journal for Computational Methods in Engineering Science and Mechanics, 7:369–380.

Stolle, D. 1982. The finite element modelling of creep and instability of large ice masses, Ph.D. Thesis, McMaster University, Hamilton.

Wan, J. 2002. Stabilized finite element methods for coupled geomechanics and multiphase flow. PhD thesis, Stanford University, CA, USA.

Wieckowski, Z., Youn, S-K. and Yeon, J-H. 1999. A particle-in-cell solution to the silo discharge problem, International Journal for Numerical Methods in Engineering, 45:1203-1225

Zienkiewicz, O.C. and Taylor, R.L. 1989. The finite element method, 4th ed, McGraw-Hill, London, Vol. 1.

Zienkiewicz, O.C. and Taylor, R.L. 1991. The finite element method, 4th ed, McGraw-Hill, London, Vol. 2.

Zienkiewicz, O. C., Rojek, J., Taylor, R. L. and Pastor M. 1998. Triangles and tetrahedral in explicit dynamic codes for solids. International Journal for Numerical Methods in Engineering, 43**:**565-583.